Compatibility of Imidazolium-Based Ionic Liquids for CO_2 Capture with Steel Alloys: a Corrosion Perspective

Maria Vittoria Diamanti[*,1], *Ursenna Vittoria Velardi*[1], *Andrea Brenna*[1], *Andrea Mele*[1], *MariaPia Pedeferri*[1], *Marco Ormellese*[1]

[1] Politecnico di Milano, Department of Chemistry, Materials and Chemical Engineering "Giulio Natta", Via Mancinelli 7, 20131 Milan, Italy

Corresponding Author

*Maria Vittoria Diamanti, Politecnico di Milano, Department of Chemistry, Materials and Chemical Engineering "Giulio Natta", Via Mancinelli 7, 20131 Milan, Italy

Tel: +390223993137, Fax: +390223993180

email: mariavittoria.diamanti@polimi.it

ABSTRACT. Ionic Liquids (ILs) could find applications in CO_2 stripping, where their use could reduce energy consumptions compared to current technologies based on amine absorption. Although preliminary studies showed potential compatibility between metallic alloys and a limited number ILs, their corrosiveness still needs to be fully assessed. This work analyzes the corrosion behavior of steel alloys in contact with several imidazolium-based ILs, changing alternatively cation and anion to highlight possible dependences of corrosion behavior on relevant groups. Potentiodynamic polarization tests were performed in all ILs considered and in water as reference. Different ILs preparation conditions were considered: after purging in nitrogen, i.e., with reduced content of oxygen and water, and after exposure to the atmosphere to restore their natural humidity and oxygen content. Results showed a reduction in the protective character of stainless steel passive film, with no clear trend related to anion composition or cation chain length. Conversely, carbon steel corrosion rate decreased compared to aqueous solutions, and a passivation effect was observed in presence of long chain cations, which was ascribed to a steric effect of adsorbed molecules.

KEYWORDS. Imidazolium; Ionic liquids; Passivation; Potentiodynamic polarization; Steel alloys

1. INTRODUCTION

CO_2 is one of the most important greenhouse gases, representing 77% of total greenhouse gas emissions [1], and is therefore responsible for the majority of infrared energy absorption that increases the temperature of the troposphere – the phenomenon known as global warming. Several CO_2 capture and storage (CCS) or conversion processes have been developed: among them, currently the most used is the post-combustion CO_2 absorption with alkanolamine solvents such as monoethanolamine (MEA), diethanolamine (DEA) and N-methyldiethanolamine (MDEA) [2-4]. This process still presents some drawbacks, such as high energy consumption for solvent regeneration, limited cyclic CO_2 loading capacity and especially corrosiveness towards metallic alloys in contact with the solvent, which limits their industrial use [5,6]. As a matter of fact, the best performing solvents in CO_2 recovery are MEA and primary amine-based ones, but they are also the most corrosive towards steels as compared with other amine solvents, since they react with CO_2 to produce carbamates – which in turn hinder the formation of a protective $FeCO_3$ layer on steel alloys. Moreover, diamines, resulting from degradation of primary and secondary amines, can be strong chelators of iron and thus promote corrosion by acid gases [7-9].

In this frame, the use of ionic liquids (ILs) is proposed as a valid alternative to the current amine-based technology [10]. The interest in ILs as fluids for CO_2 capture and for important applications such as natural gas sweetening relies upon the capability of some ILs of retaining significant amounts of CO_2 while showing limited absorption properties towards hydrocarbons, methane in particular [11]. Moreover, these solvents would provide high efficiency and cyclic loading capacity thanks to a low vapour pressure, which allows full regeneration and reuse without losses in gas streams, and high temperature and chemical stability; regeneration itself would require less energy, due to a different absorption mechanism compared with amines

[12,13]. The latter point is of pivotal importance in view of possible applications of ILs technology on the industrial scale. As recently stressed, one of the major issues against the use of ILs is their high cost. However, Papatryfon et al [14] pointed out that the capability of ILs based absorption units of undergoing sequential duty cycles without need to replenish should be accounted for in the economic comparison with the currently used amine based processes that, conversely, require frequent shut down steps. A careful evaluation of the costs associated to ILs use on industrial scale is thus mandatory before discarding ILs as alternative materials for CO_2 sorption.

The direct contact of ILs based sorbents to the metallic components of a plant – pipes, reactors, heat exchangers, desorption chambers etc. – calls for a deep understanding of the compatibility between ILs and metallic materials. Some studies have been performed, mostly focusing on the use of ILs as corrosion inhibitors [15-19], or on the development of new protection solutions for highly reactive metals, such as magnesium or aluminium: this is based on the formation of conversion coatings some tens or hundreds of nanometres thick, rich in phosphates and other ions that show passivating behavior towards such metals [20-22]. On the other hand, fewer studies deal with their corrosiveness towards metals and other materials, from steel alloys to copper and magnesium, to carbon [23-31]. In this respect, common examples of ILs tested include chloride-rich ones, which are clearly unsuitable for the purpose and induce harsh corrosion conditions, being chlorides extremely aggressive towards active-passive metals [27,28]. In the present paper we start a systematic study of the corrosion properties of some alkyl-methylimidazolium ILs [C_nC_1Im] with fluorinated anions on steel alloys. As a starting step of a long term project, we report here on the role played by different alkyl chain lengths bound to the imidazolium ring, and by three different anions, bis(trifluoromethylsulfonyl)imide ([TFSI]),

tetrafluoroborate ([BF_4]) and hexafluorophosphate ([PF_6]). This class of ILs showed potential capability of CO_2 capture with good performances [32-34]. The main purpose of this work is to provide some paradigmatic examples and testing protocols of the corrosion profile of pure ILs with CO_2 capture capabilities on steel alloys, as simple systems mimicking the conditions of an industrial plant. Although these systems have been thoroughly investigated from the structural and physicochemical point of view, they have received only marginal attention in the evaluation of their potential corrosiveness towards metallic facilities [35-38]. On account of their potential industrial importance, a systematic study over the corrosion resistance of the typical metals used in existing plants is required to fill this gap. Previous studies on carbon steel pointed out limited corrosiveness of 1-butyl-3-methylimidazolium and 1-ethyl-3-methylimidazolium tetrafluoroborate, also in co-presence of amines and CO_2 [35]; some imidazolium-based ILs are even considered for applications as corrosion inhibitors, due to their adsorption and consequent formation of a protective film on the steel surface [15-18]. More specific and wider spectrum studies showed a correlation between an increase in alkyl chain length and inhibitive properties of 1-alkyl-3-methylimidazolium tricyanomethanide, and associated localized corrosion events with the dissolution of manganese sulfide impurities [36,37]. Yet, such studies are far from completing the picture of ILs corrosiveness, concerning both potential ILs compositions and preparation conditions – e.g., water content, oxygen content, CO_2 content, understanding of the corrosion mechanisms on different metallic alloys.

2. EXPERIMENTAL METHODS

Imidazolium-based ILs were purchased from IOLITEC GmbH, with declared purity higher than 99%. Different formulations were chosen, in order to observe the possible influence of either

anion composition or cation alkyl chain length. The following ILs were selected: 1-butyl-3-methylimidazolium tetrafluoroborate [C_4C_1Im][BF_4], 1-butyl-3-methylimidazolium hexafluorophosphate [C_4C_1Im][PF_6], 1-butyl-3-methylimidazolium bis(trifluoromethylsulfonyl)imide [C_4C_1Im][TFSI] to test the effect of anion composition; 1-butyl-3-methylimidazolium [C_4C_1Im], 1-hexyl-3-methylimidazolium [C_6C_1Im], and 1-methyl-3-octylimidazolium [C_8C_1Im], all combined with [TFSI] anion or with [PF_6] anion to test the effect of alkyl chain. Molecular structures are summarized in Figure 1; the main physical properties are reported in Table 1.

<Figure 1>

<Table 1>

All ILs were preliminarily treated in vacuum at 70°C for five hours in order to minimize water content, which was then measured by Karl Fischer titration. ILs were stored under nitrogen atmosphere in a drybox in order to keep water and oxygen content as low as possible. Initial water contents resulted to be between 100 and 1000 ppm, being lower in [TFSI] based ILs; this demonstrates a hydrophilic character of the selected ILs, which tend to absorb water by simple contact with the atmosphere, as happened when preparing them for the measurements. Corrosion tests were performed on the dehydrated and purged ILs: water values measured before and after potentiodynamic polarization tests were very similar, indicating that the corrosion tests were performed in homogeneous conditions.

Corrosion tests were then repeated on ILs after aeration by exposure to the atmosphere for 48 hours, in order to restore their natural oxygen content and humidity, which increased by 20% in

[TFSI] based liquids, by 100% in [PF_6] ones and by 1 order of magnitude in [BF_4] ILs, showing the difference in hydrophilicity induced by the three anions.

The corrosiveness of ILs was evaluated on two common steel alloys used in industrial plants and facilities: stainless steel UNS S31600 (SS) and carbon steel API 5L X52 (CS) with compositions given in Table 2. This was aimed at evaluating the potential interaction of ILs with both an active metal alloy, i.e., generally undergoing corrosion in most environments, and a passive one, i.e., a metal able to shield its surface from the environment by growing a thin and compact oxide film with protective behavior.

<Table 2>

Potentiodynamic polarization tests were performed in a small volume Teflon cell (hereon, minicell: Figure 2), containing 3 ml of solution on an exposed anodic area of 0.785 cm^2. An Ag/AgCl reference electrode was used, in the form of an AgCl plated Ag wire with 0.2 mm diameter, purchased from A-M Systems. An activated titanium wire was used as counter electrode. Potentiodynamic tests were performed by applying a scan rate of 10 mV/min; the applied voltage of anodic curves ranged from open circuit potential (OCP) to +1.1 V Ag/AgCl on passive steels, from OCP to OCP+0.3 V on active steels; cathodic curves were recorded from OCP to -1 V Ag/AgCl. Tests were carried out in the presence of all ILs selected as well as of tap water, which was used as comparison. The main properties of the tap water used are reported in Table 3. All tests were repeated at least twice to ensure data reproducibility, and in case of disagreement more replicates were performed: if not further commented, the two replicates can be considered as coincident and only one of the two curves is shown.

<Figure 2>

<Table 3>

3. RESULTS AND DISCUSSION

In the following paragraph, results of electrochemical tests are divided into sections according to the different parameters analyzed. First, a brief assessment of the minicell reliability is summarized, followed by a series of analyses describing the cathodic and anodic behavior of the metals considered; finally, the influence of environmental parameters – IL anion formulation, cation chain length, presence of water – on the metal corrosion attitude is presented.

3.1 Minicell reliability

In order to ensure the reliability of the minicell built on purpose for this experimental work, several potentiodynamic tests were performed on both steels in tap water. The metal sample was subjected to anodic polarization as well as to cathodic polarization (data not shown). Results were compared with typical anodic and cathodic characteristics recorded in standard test conditions, according to corrosion tests standards ASTM G5 [39] and G61 [40]. As expected, discrepancies were observed between numerical values of the limiting current density of oxygen in the two systems; still, open circuit potential values were comparable, and multiple anodic and cathodic curves recorded in the small volume cell showed excellent repeatability. These observations allow to consider the minicell as reliable, although numerical results may not be compared with those obtained in standard cells.

3.2 Effect of ILs on cathodic process

Figure 3 reports the cathodic curves recorded on both steels in aerated ILs, as a function of anion and cation formulation; curves not shown present similar trends and values.

The cathodic process shows similar cathodic current density on both stainless steel and carbon steel, dispersed in a range of less than one order of magnitude; values measured on stainless steel in water also lie in the same range. It is therefore assumed that the limiting current density observed is related to oxygen reduction. It is interesting to notice that the corrosion potential of carbon steel in ILs approaches that of stainless steel, increasing at least by 400 mV with respect to values measured in tap water.

<Figure 3>

3.3 Effect of ILs formulation on anodic behavior of CS and SS

The electrochemical behavior of stainless steel and carbon steel in ILs with the common cation 1-butyl-3-methylimidazolium [C_4C_1Im] and the three different anions BF_4, PF_6 and TFSI was evaluated through anodic polarization. Results are reported in Figure 4, which also includes tests performed in water to provide a comparison with an environment of known aggressiveness.

<Figure 4>

The electrochemical behavior of stainless steel in the ILs tested is passive. In particular, in presence of [C_4C_1Im][BF_4] the current density recorded in the passivity region – which is proportional to the passivity current density – is comparable to that obtained in H_2O and smaller than that presented in other ILs.

Although there is a slight discrepancy – 200 mV – in open circuit potentials (OCPs) of stainless steel measured in dry $[C_4C_1Im][PF_6]$ and after the exposure of the IL to air, both curves show a passive behavior with same current density in the passivity region. Data collected on both steel alloys in $[C_4C_1Im][BF_4]$ and $[C_4C_1Im][PF_6]$ show high repeatability, whereas in $[C_4C_1Im][TFSI]$ data dispersion makes the evaluation of the electrochemical behavior more difficult. This may be a result of a complex interaction between metal alloys and the TFSI anion.

On the other hand, the behavior of carbon steel in $[C_4C_1Im][BF_4]$ is clearly active. Only in the case of $[C_4C_1Im][PF_6]$ carbon steel shows a passive behavior, although with higher current densities compared to stainless steel in the same solution, as highlighted in Figure 5. Moreover, open circuit potentials of carbon steel in $[C_4C_1Im][PF_6]$ are higher than those observed in $[C_4C_1Im][BF_4]$ and $[C_4C_1Im][TFSI]$, indicating an increase in the alloy nobility.

<Figure 5>

These data allow to draw some preliminary conclusions on the influence of anion composition on ILs corrosiveness. Stainless steel showed a clearly passive behavior in all ILs tested, with corrosion current densities in the passive range – and therefore corrosion rate – increasing in the following order:

water < $[BF_4]_{dry,\ aerated}$ ~ $[TFSI]_{aerated}$ < $[TFSI]_{dry}$ ~ $[PF_6]_{dry,\ aerated}$

Unfortunately, $[BF_4]$ and [TFSI] also resulted in a high corrosion rate on carbon steel, although slightly lower than that observed in water: the higher corrosion potential could have suggested higher nobility, which is confirmed by a decrease in cathodic current density – proportional to corrosion rate – on active carbon steel, but the effect was not sufficient to protect the metal from

intense generalized corrosion. Conversely, [PF_6] anions produced a positive effect on carbon steel corrosion resistance, resulting in metal passivation. On the basis of these results we chose to perform a new series of analyses by changing the alkyl chain length in combination with both [TFSI] and [PF_6] anions, the former chosen on the basis of its superior CO_2 storage capacity, the latter on the basis of its superior protectiveness towards metal alloys and good CO_2 storage capacity [12,32].

3.4 Effect of ILs alkyl chain length on anodic behavior of CS and SS

Figure 6 presents the anodic processes of stainless steel and carbon steel in TFSI-based ILs with different alkyl chain length, compared with those observed in water; Figure 7 shows analogous results for PF_6-based ILs.

An interesting observation concerns the dispersion of experimental results in presence of [TFSI]. Conversely to what experienced in presence of [BF_4] and [PF_6] anions, a high dispersion of data was observed, with curves recorded in identical electrolytes leading to different results. This suggests a complex effect of [TFSI] on the steel alloys considered, leading in some cases to a protective effect while confirming its poor protectiveness in most tests. This is highlighted in Figure 6B, where two different curves are presented for carbon steel anodic polarization in [C_4C_1Im][TFSI] and [C_6C_1Im][TFSI] electrolytes: in both cases, one curve shows a beginning of passivation, while the other is typical of a clearly active material.

<Figure 6>

This can be ascribed to the reaching of a borderline condition for passivation, and this consideration is proved by the fact that for longer alkyl chain [C_8C_1Im] passivation is actually

achieved on carbon steel. In fact, the length of the cation alkyl chain influences its corrosion behavior: carbon steel shows an active behavior in $[C_4C_1Im][TFSI]$ and $[C_6C_1Im][TFSI]$ and a prominently passive one in $[C_8C_1Im][TFSI]$. The transition from active to passive behavior is ascribed to a filming effect of ILs with long alkyl chain, which protect the steel surface in a similar fashion to the working principle of a corrosion inhibitor, as already proposed in previous works [35-37]. Concerning stainless steel, an inverse proportionality between chain length and protective character of the passive film is evidenced, which contrasts with all other experimental behaviors observed; yet, considering data dispersion in the presence of [TFSI] based ILs and the limited variation observed, it is possible to consider the effect not relevant.

Owing to the limited reliability of results obtained in presence of [TFSI], tests on the influence of alkyl chain length were repeated on ILs containing the $[PF_6]$ anion in aerated conditions (Figure 7).

<Figure 7>

Interestingly, in this case the C_4 chain is already sufficient to induce a passivation effect on carbon steel. Yet, conversely to what observed in presence of [TFSI], current densities recorded do not decrease below 1 A/m^2, therefore providing a limited surface protection. On stainless steel, which is clearly passive in all conditions tested, an increased resistance of the passive film is observed in presence of C_8 chain lengths, with a decrease in anodic current densities by 30%.

3.5 Effect of water content

Concerning the effect of water content on stainless steel, UNS S31600 presented a passive behavior in all TFSI and PF_6-based ILs, with values of current density in the passive region higher

than those measured in water; furthermore, current densities were higher in dehydrated ILs than those measured in ILs in equilibrium with atmospheric water and oxygen. This trend can be justified by the fact that dehydrated ILs contain a smaller amount of oxygen and water, which are needed to form the passivation film on the metal, therefore the equilibrium passive film may show a reduced barrier effect.

3.6 Discussion

To summarize the experimental observations here presented, Table 4 reports the passivity current densities observed by potentiodynamic polarization of carbon steel and on stainless steel in presence of all ILs tested, considering aerated conditions as more adherent to possible applications – where controlling ILs oxygen and water content would require technological solutions incompatible with current facilities. Figure 8 reports optical micrographs of stainless and carbon steel surfaces before and after the test, in order to evidence corrosion attacks.

The contact with any of the ILs studied causes a decrease in the protective character of stainless steel passive film: this can be ascribed to the low content of water, which is crucial to allow surface passivation. As abovementioned, this hypothesis is supported by the fact that ILs subjected to drying provoked a further increase in corrosion current densities. Yet, no corrosion attack is visible on the surface (Figure 8-left), coherently with the passive behavior still observed on the metal in spite of the large current densities involved.

<Table 4>

On the other hand, carbon steel experienced the formation of a passive film in the presence of [TFSI] combined with long alkyl chain lengths, or [PF_6] with all cations considered. A nobilitation of its free corrosion potential by more than 0.5 V was also observed in all conditions, going from -0.69 V to approximately -0.1 V, thus reaching values close to those of stainless steel (-0.14 V in water, ~ 0 V in ILs). The passivation of carbon steel was ascribed to a filming behavior of ILs, through a proposed mechanism of adsorption on the metal surface that would hinder the metal surface from being in contact with oxygen and water, responsible for the corrosion reactions. This also implies an improvement in filming behavior with increasing length of the IL alkyl chain: such condition was actually observed, as proved by the decrease in the extension of corrosion attacks on the surface of carbon steel by increasing chain length from C_4 to C_6 and finally to C_8 (Figure 8-right).

Among the solutions considered, [C_8C_1Im][TFSI] is the IL that allows the best combination of CO_2 capture capability and low corrosiveness; yet, the higher repeatability of experimental tests performed in presence of PF_6 anion indicate that the best candidate in terms of compatibility with steel alloys would be [C_8C_1Im][PF_6]. Such considerations need further expansion of experimental tests in presence of water/ILs mixtures or amines/ILs mixtures to simulate the actual formulations of solvents currently considered for CO_2 capture and storage applications. In fact, the presence of water has already proved to change the outcomes of metal-electrolyte interactions by accelerating or reducing reaction rates, as emerged from works on the electrodeposition of chromium from ILs based electrolytes [41-43].

<Figure 8>

4. CONCLUSIONS

This work presented a systematic analysis of the impact of alkyl-methylimidazolium ionic liquids of different composition on the durability of steel alloys that may work in contact with such substances, specifically, a stainless steel and a carbon steel. A screening method is proposed based on potentiodynamic polarization tests in a small volume cell (minicell), which allows to reduce the used IL volume at minimum while still performing the test on a significant area of metal. The investigation showed how the composition of the IL has a crucial role in determining the corrosiveness of the IL itself towards the two steels, for what concerns both the anion and the cation, and different effects were pointed out depending on the IL-metal combination. In particular, carbon steel is not compatible with use in presence of ILs with short alkyl chain, and in particular with the $[BF_4]$ anion, while at increasing chain lengths it tends to passivate, therefore presenting good corrosion resistance; the best compatibilities were obtained with $[C_8C_1Im][PF_6]$ and $[C_8C_1Im][TFSI]$. On the other hand, the contact between ILs and stainless steel presents in general a detrimental effect with respect to the typical behavior of stainless steel in water, which was ascribed to the lack of water needed to maintain the passive film protective. In fact, water plays a fundamental role in steel corrosion, as the presence of absorbed CO_2 also does: therefore, this first screening will require further investigations in ternary systems composed by ILs, water and CO_2.

REFERENCES

[1] IPCC Climate Change 2007 Assessment report 4: Synthesis report, p. 36.

[2] Khoo H.H.; Tan, R.B.H. Carbon capture and utilization: Preliminary life cycle CO_2, energy, and cost results of potential mineral carbonation *Environ. Sci. Technol*. **2006**, *40*, 4016–4024.

[3] D'Alessandro, D.M.; Smit, B.; Long, J.R. Carbon dioxide capture: Prospects for new materials. *Angew. Chem. Int.* **2010**, *49*, 6058–6082.

[4] Boroojerdi, S.; Erfani, A.; Dehghani, A; Hamzavi, A; Abyaneh, M.Z. Simulation-assisted study of temperature, pH, energy consumption and separation performance for different amines and amine mixtures in CO_2 removal unit of ammonia plant. *Petroleum and Coal* **2013**, *55*, 273-282.

[5] Wattanaphan, P.; Sema, T.; Idem, R.; Liang, Z.; Tontiwachwuthikul, P. Effects of flue gas composition on carbon steel (1020) corrosion in MEA-based CO_2 capture process. *Int. J. Greenh. Gas Control* **2013**, *19*, 340-349.

[6] Rawat, J.; Rao, P.V.C.; Choudary, N.V. Controlling corrosion in amine treatment units. *GAS* **2011**, 1000410.

[7] Soosaiprakasam, I.R.; Veawab, A. Corrosion and polarization behavior of carbon steel in MEA-based CO_2 capture process. *Int. J. Greenh. Gas Control* **2008**, *2*, 553-562.

[8] Dupart, M.S.; Bacon, T.R.; Edwards, D.J. Part1-Understanding corrosion in alkanolamine gas treating plants. *Hydrocarbon Proc.* **1993**, (April), 75-80.

[9] Dupart, M.S.; Bacon, T.R.; Edwards, D.J. Part2-Understanding corrosion in alkanolamine gas treating plants. *Hydrocarbon Proc.* **1993**, (May), 89-94.

[10] Karadas, F.; Atilhan, M.; Aparicio, S. Review on the use of ionic liquids (ILs) as alternative fluids for CO_2 capture and natural gas sweetening. *Energy Fuels* **2010**, *24*, 5817-582

[11] Hasib-ur-Rahman, M.; Siaj, M.; Larachi, F. Ionic liquids for CO_2 capture – Development and progress. *Chem. Eng. Process.* **2010**, *49*, 313-322

[12] Zhang, X.; Zhang, X. Dong, H.; Zhao. Z.; Zhang, S.; Huang, Y. Carbon capture with ionic liquids: overview and progress. *Energy Environ. Sci.* **2012**, *5*, 6668-6681.

[13] Ashassi-Sorkhabi, H.; Es'haghi, M. Corrosion inhibition of mild steel in acidic media by [C4]Br Ionic liquid. *Mater. Chem. Phys.* **2009**, *114*, 267–271.

[14] Papatryfon, X. L.; Heliopoulos, N. S.; Molchan, I. S.; Zubeir, L. F.; Bezemer, N. D.; Arfanis, M. K.; Kontos, A. G.; Likodimos, V.; Iliev, B.; Romanos, G. E.; Falaras, P.; Stamatakis, K.; Beltsios, K. G.; Kroon, M. C.; Thompson, G. E.; Klöckner, J.; Schubert, T.J.S. CO_2 capture efficiency, corrosion properties, and ecotoxicity evaluation of amine solutions involving newly synthesized ionic liquids. *Ind. Eng. Chem. Res.* **2014**, *53*, 12083-12102.

[15] Zhang, Q.B.; Hua, Y.X. Corrosion inhibition of mild steel by alkylimidazolium ionic liquids in hydrochloric acid. *Electrochim. Acta* **2009**, *54*, 1881–1887.

[16] Hasib-ur-Rahman, M.; Larachi, F. Prospects of using room-temperature ionic liquids as corrosion inhibitors in aqueous ethanolamine-based CO_2 capture solvents. *Ind. Eng. Chem. Res.* **2013**, *52*, 17682−17685.

[17] Likhanova, N.; Domínguez-Aguilar, M.A.; Olivares-Xometl, O.; Nava-Entzana, N.; Arce, E.; Dorantes, E. The effect of ionic liquids with imidazolium and pyridinium

cations on the corrosion inhibition of mild steel in acidic environment. *Corros. Sci.* **2010**, *52*, 2088–2097.

[18] Uerdingen, M.; Treber, C.; Balser, M.; Schmitt, G.; Werner, C. Corrosion behaviour of ionic liquids. *Green Chem*. **2005**, *7*, 321–325.

[19] Atta, A.M.; El-Mahdy, G.A.; Al-Lohedan, H.A.; Ezzat, A.R.O. A new green ionic liquid-based corrosion inhibitor for steel in acidic environments. *Molecules* **2015**, *20,* 11131-11153.

[20] Huang, P.; Latham, J.A.; MacFarlane, D.R.; Howlett, P.C.; Forsyth, M. A review of ionic liquid surface film formation on Mg and its alloys for improved corrosion performance. Electrochim. Acta 2013, 110, 501-510.

[21] Huang, P.; Howlett, P.C.; Forsyth, M. Electrochemical etching of AA5083 aluminium alloy in trihexyl(tetradecyl)phosphonium bis(trifluoromethylsulfonyl)amide ionic liquid. Corros. Sci. 2014, 80, 120-127.

[22] Chong, A.L.; Forsyth, M.; MacFarlane, D.R. Novel imidazolinium ionic liquids and organic salts. Electrochim. Acta 2015, 159, 219-226.

[23] Chatterjee, S.; Carter, R.; Oakes, L.; Erwin, W.R.; Bardhan, R.; Pint, C.L. Electrochemical and corrosion stability of nanostructured silicon by graphene coatings: Toward high power porous silicon supercapacitors. *J. Phys. Chem. C* **2014**, *118*, 10893-10902.

[24] Perissi, I.; Bardi, U.; Caporali, S.; Fossati, A.; Lavacchi, A.; Vizza, F. Ionic liquids: Electrochemical Investigation on corrosion activity of ethyl-dimethyl-propylammonium bis(trifluoromethylsulfonyl)imide at high temperature. *Russian J. Electrochem.* **2012**, *48*, 434–441.

[25] Pisarova, L.; Gabler, C.; Dörr, N.; Pittenauer, E.; Allmaier, G. Thermo-oxidative stability and corrosion properties of ammonium based ionic liquids. *Tribol. Int*. **2013**, *46*, 73-83.

[26] Wang, Y-C.; Lee, T-C.; Lin, J-Y.; Chang, J-K.; Tseng, C-M. Corrosion properties of metals in dicyanamide-based ionic liquids. *Corros. Sci.* **2014**, *78*, 81-88.

[27] Lin, P-C.; Sun, I-W.; Chang, J-K.; Su, C-J.; Lin, J-C. Corrosion characteristics of nickel, copper, and stainless steel in a Lewis neutral chloroaluminate ionic liquid. *Corros. Sci*. **2011**, *53*, 4318–4323.

[28] Tseng, C-H.; Chang, J-K.; Chen, J-R.; Tsai, W.S.; Deng, M-J.; Sun, I-W. Corrosion behaviors of materials in aluminum chloride–1-ethyl-3-methylimidazolium chloride ionic liquid. *Electrochem. Commun.* **2010**, *12*, 1091–1094.

[29] Zheng, J.; Moganty, S.S.; Goonetilleke, P.C.; Baltus, R.E.; Roy, D. A comparative study of the electrochemical characteristics of [Emim+][BF4-] and [Bmim+][BF4-] ionic liquids at the surfaces of carbon nanotube and glassy carbon electrodes. *J. Phys. Chem. C* **2011**, *115*, 7527-7537.

[30] Mahapatro, A.; Kumar, S.S. Determination of ionic liquid and magnesium compatibility via microscopic evaluations. *J. Adv. Microscopy Res.* **2015**, *10*, 89-92.

[31] Oishi, M.; Ichistubo, T.; Okamoto, S.; Toyoda, S.; Matsubara, E.; Nohira, T.; Hagiwara, R. Electrochemical behavior of magnesium alloys in alkali metal-tfsa ionic liquid for magnesium-battery negative electrode. *J. Electrochem. Soc.* **2014**, *161*, A943-A947.

[32] Lei, Z.; Dai, C.; Chen, B. Gas solubility in ionic liquids. *Chem. Rev*. **2014**, *114*, 1289-1326.

[33] Cadena, C.; Anthony, J.L.; Shah, J.K.; Morrow, T.I.; Brennecke, J.F.; Maginn, E.J. Why is CO_2 so soluble in imidazolium-based ionic liquids? *J. Am. Chem. Soc.* **2004**, *126*, 5300-5308.

[34] Aki, S.N.V.K.; Mellein, B.R.; Saurer, E.M.; Brennecke, J.F. High-pressure phase behavior of carbon dioxide with imidazolium-based ionic liquids. *J. Phys. Chem. B* **2004**, *108*, 20355-20365.

[35] Hasib-ur-Rahman, M.; Bouteldja, H.; Fongarland, P.; Siaj, M.; Larach, F. Corrosion behavior of carbon steel in alkanolamine/room-temperature ionic liquid based CO_2 capture systems. *Ind. Eng. Chem. Res.* **2012**, *51*, 8711−8718.

[36] Molchan, I.S.; Thompson, G.E.; Lindsay, R.; Skeldon, P.; Likodimos, V.; Romanos, G.E.; Falaras, P.; Adamova, G.; Iliev, B.; Schubert, T.J.S. Corrosion behaviour of mild steel in 1-alkyl-3-methylimidazolium tricyanomethanide ionic liquids for CO_2 capture applications. *RSC Adv.* **2014,** *4*, 5300-5311.

[37] Molchan, I.S.; Thompson, G.E.; Skeldon, P.; Lindsay, R.; Walton, J.; Kouvelos, E.; Romanos, G. E.; Falaras, P.; Kontos, A. G.; Arfanis, M.; Siranidi, E.; Zubeir, L. F.; Kroon, M. C.; Klöckner, J.; Iliev, B.; Schubert, T.J.S. Microscopic study of the corrosion behaviour of mild steel in ionic liquids for CO_2 capture applications. *RSC Adv.* **2015,** *5*, 35181-35194.

[38] Lebedeva, O.; Jungurova, G. Zakharov, A.; Kultin, D.; Chernikova, E.; Kustov, L. Water as inhibitor of metal corrosion in hydrophobic ionic liquids. *J. Phys. Chem. C* **2012**, *116*, 22526-22531.

[39] ASTM standard G5, 2013, Standard reference test method for making potentiodynamic anodic polarization measurements. In: *Annual Book of ASTM Standards*, vol. 03.02,

ASTM International, West Conshohocken, PA, 2013, DOI: 10.1520/G0005, www.astm.org.

[40] ASTM standard G61, 1986 (R 2014), Standard test method for conducting cyclic potentiodynamic polarization measurements for localized corrosion susceptibility of iron-, nickel-, or cobalt-based alloys. In: *Annual Book of ASTM Standards*, vol. 03.02, ASTM International, West Conshohocken, PA, 2014, DOI: 10.1520/G0061, www.astm.org.

[41] Surviliene, S.S.; Eugénio, S.; Vilar, R. Chromium electrodeposition from [BMIm][BF4] ionic liquid. J. Appl. Electrochem. 2011, 41, 107-114.

[42] McCalman, D.C.; Sun, L.; Zhang, Y.; Brennecke, J.F.; Maginn, E.J.; Schneider, W.F. Speciation, conductivities, diffusivities, and electrochemical reduction as a function of water content in mixtures of hydrated chromium chloride/choline chloride. J. Phys. Chem. B, 2015, 119, 6018-6023.

[43] Sun, L.; Brennecke, J.F. Characterization of Imidazolium Chloride Ionic Liquids Plus Trivalent Chromium Chloride for Chromium Electroplating. Ind. Eng. Chem. Res. 2015, 54, 4879-4890.

FIGURE CAPTIONS

Figure 1. Molecular structures of ILs investigated; the variation of anions on a common cation and of cations on a common anion is highlighted.

Figure 2. Minicell designed for electrochemical tests.

Figure 3. Examples of cathodic polarization curves of stainless steel UNS S31600 (SS) and carbon steel API 5L X52 (CS) recorded in different electrolytes. Point lines: water, dashed lines: SS, solid lines: CS. A) SS and CS in different IL anions: $[C_4C_1Im][TFSI]$, in green; $[C_4C_1Im][PF_6]$, in orange; $[C_4C_1Im][BF_4]$, in black. B) CS in different IL cations: from dark to light green with increasing alkyl chain length, $[C_4C_1Im][TFSI]$; $[C_6C_1Im][TFSI]$; $[C_8C_1Im][TFSI]$.

Figure 4. Anodic polarization curves of A) stainless steel UNS S31600 (SS) and B) carbon steel API 5L X52 (CS) recorded in different ILs based on $[C_4C_1Im]$ cation. Point lines: water, dashed lines: dry ILs, solid lines: aerated ILs. $[C_4C_1Im][TFSI]$ in green; $[C_4C_1Im][PF_6]$ in orange; $[C_4C_1Im][BF_4]$ in black.

Figure 5. Anodic polarization curves of stainless steel UNS S31600 (SS, dashed line) and carbon steel API 5L X52 (CS, solid line) recorded in $[C_4C_1Im][PF_6]$.

Figure 6. Anodic polarization curves of A) stainless steel UNS S31600 (SS) and B) carbon steel API 5L X52 (CS) recorded in ILs based on [TFSI] anion. Point lines: water, dashed lines: dry ILs, solid lines: aerated ILs, from dark to light green with increasing alkyl chain length, $[C_4C_1Im][TFSI]$; $[C_6C_1Im][TFSI]$; $[C_8C_1Im][TFSI]$.

Figure 7. Anodic polarization curves of A) stainless steel UNS S31600 (SS) and B) carbon steel API 5L X52 (CS) recorded in ILs based on $[PF_6]$ anion: from dark to light orange with increasing alkyl chain length, $[C_4C_1Im][TFSI]$; $[C_6C_1Im][TFSI]$; $[C_8C_1Im][TFSI]$.

Figure 8. Optical micrographs recorded on stainless steel (left) and carbon steel (right) before and after potentiodynamic tests. Darker spots correspond to corroded areas.

Figure 1

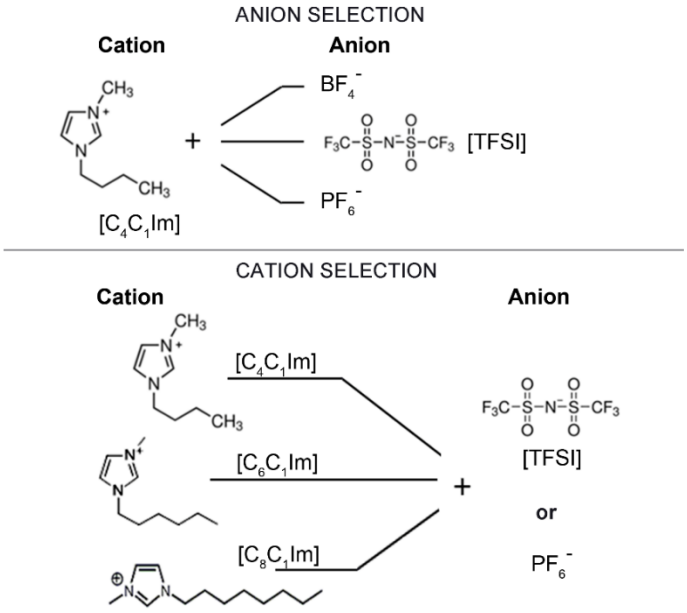

Figure 2

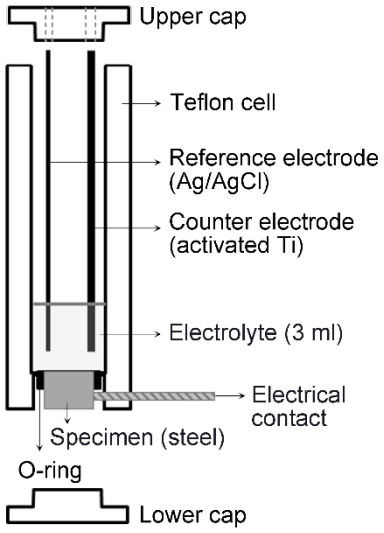

Figure 3

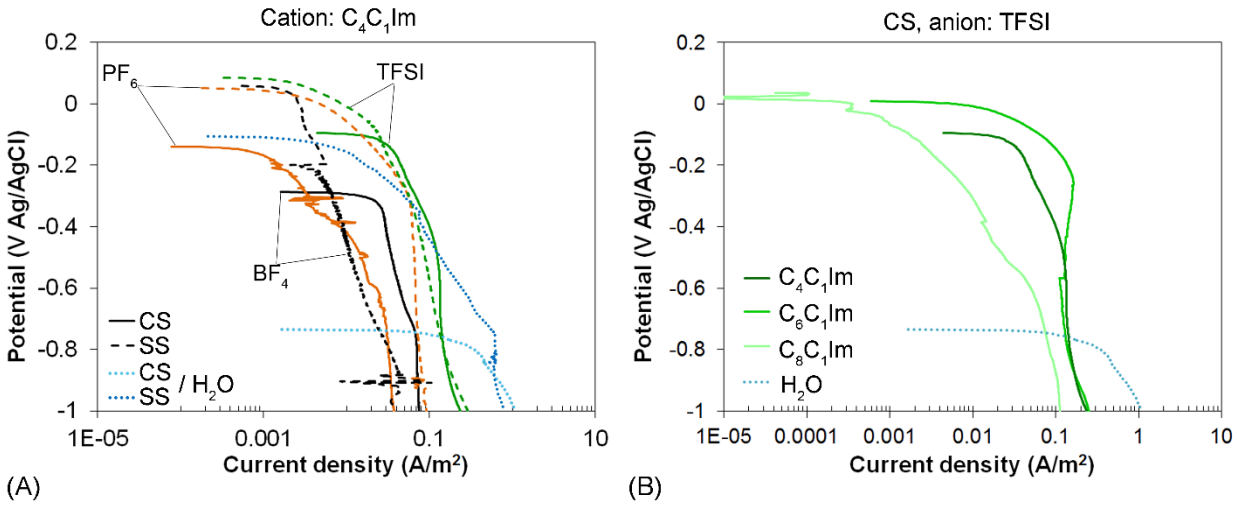

Figure 4

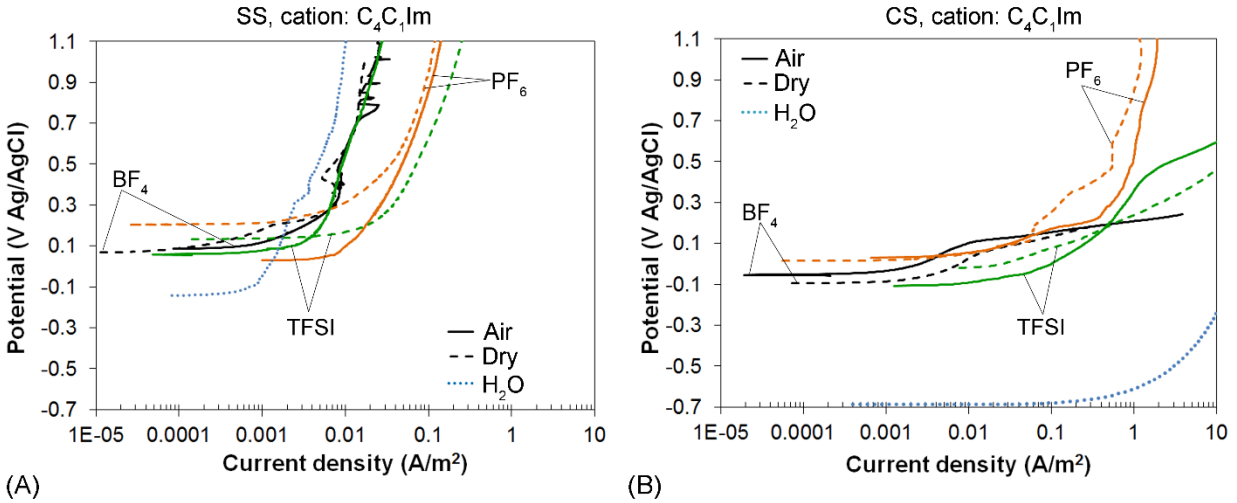

Figure 5

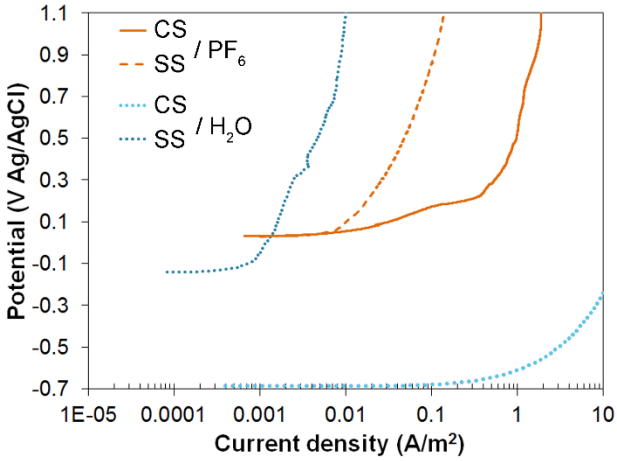

Figure 6

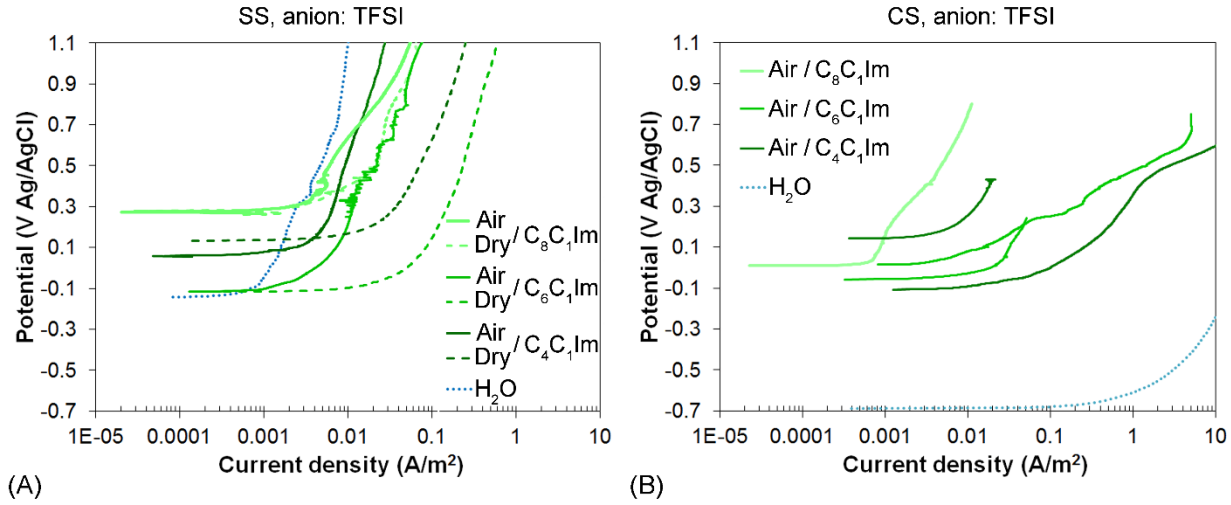

Figure 7

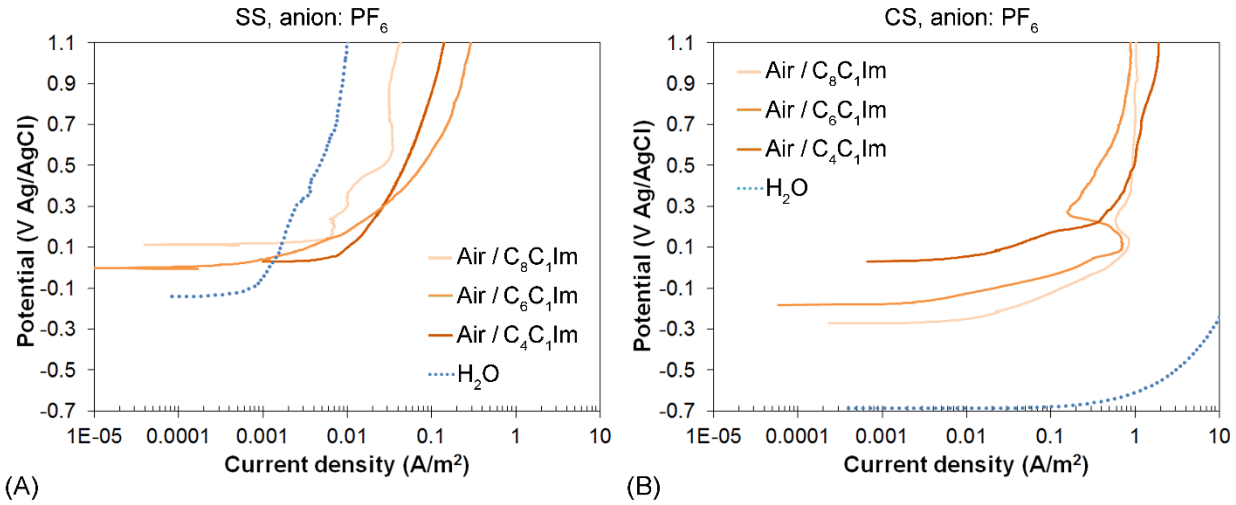

Figure 8

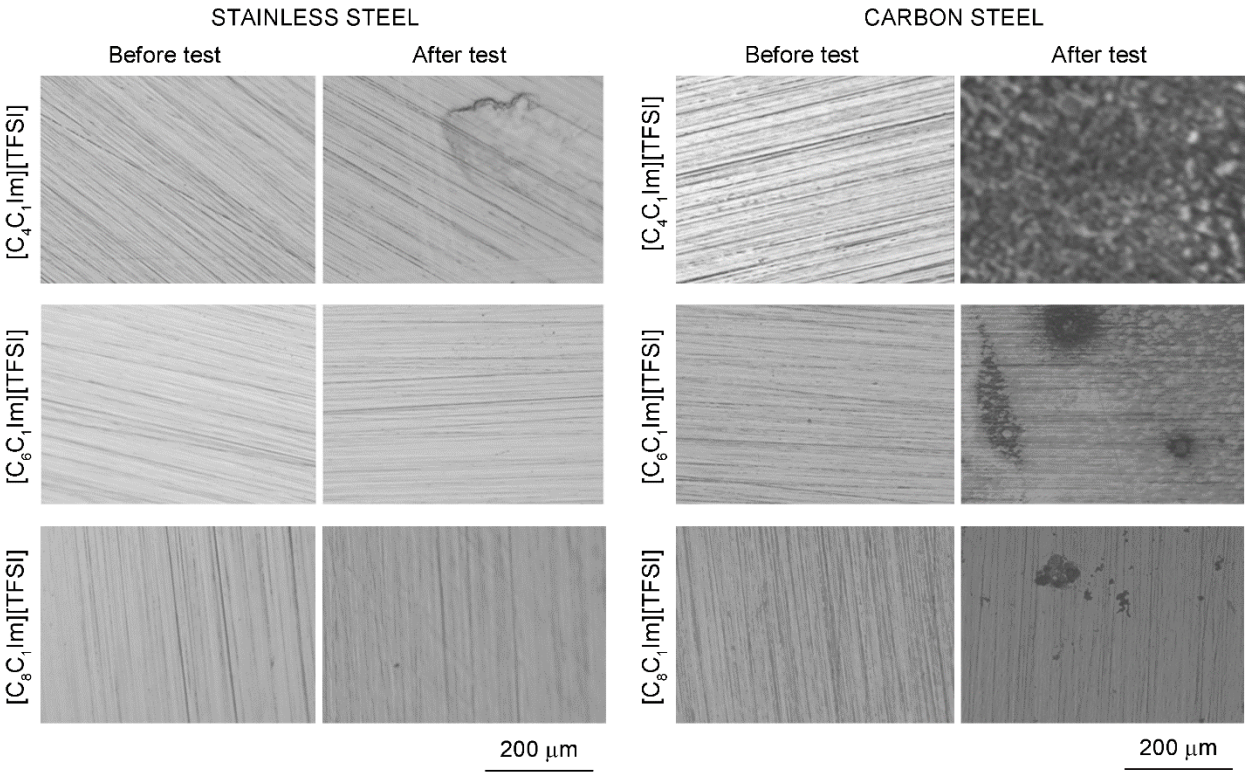

Table 1. Physical data of ILs investigated, as provided by the producer.

IL	$[C_4C_1Im]$ $[TFSI]$	$[C_6C_1Im]$ $[TFSI]$	$[C_8C_1Im]$ $[TFSI]$	$[C_4C_1Im]$ $[BF_4]$	$[C_4C_1Im]$ $[PF_6]$	$[C_6C_1Im]$ $[PF_6]$	$[C_8C_1Im]$ $[PF_6]$
purity	>99%	>99%	>99%	>99%	>99%	>99%	>99%
density (g/ml)	1.43	1.36	1.32	1.17	1.37	1.26	1.20
viscosity (cP)	61.41	68	104	108	285	707	1052
water (ppm)	50	100	40	150	120	190	180

Table 2. Composition of steel alloys used, % by mass.

	C	**Si**	**Mn**	**S**	**P**	**Cr**	**Ni**	**Mo**
UNS S31600	<0.08%	<0.75%	<2.00%	<0.03%	<0.045%	17.8%	9.8%	2.7%
API 5L X52	<0.07%	<0.07%	<0.33%	<0.008%	<0.017%	-	-	-